Inorganic Chemistry Communications 108 (2019) 107496

Contents lists available at ScienceDirect

Inorganic Chemistry Communications

journal homepage: www.elsevier.com/locate/inoche

Editorial

Novel series of nanosized mono- and homobi-nuclear metal complexes of sulfathiazole azo dye ligand: Synthesis, characterization, DNA-binding affinity, and anticancer activity

Abdalla M. Khedr[a,b], Hoda El-Ghamry[a,b], Mohammed A. Kassem[a,c,*], Fawaz A. Saad[a], Nizar El-Guesmi[a,d]

[a] Department of Chemistry, Faculty of Applied Science, Umm Al-Qura University, Makkah, Saudi Arabia
[b] Chemistry Department, Faculty of Science, Tanta University, Tanta, Egypt
[c] Chemistry Department, Faculty of Science, Benha University, Benha, Egypt
[d] Chemistry Department, Faculty of Science, Monastir University, Tunisia

ARTICLE INFO

Keywords:
Sulfathiazole azo
Anticancer activity
Nanosized complexes
DNA binding modes

ABSTRACT

Novel five nanosized mono- and homobi-nuclear complexes of 4-(2,4-dihydroxy-5-formylphen-1-ylazo)-N-thiazol-2-yl-benzenesulfonamide (H_2L) ligand were synthesized for developing new anticancer agents. H_2L was prepared by coupling the diazonium salt of 2-(p-aminobenzenesulfonamido)thiazole with 2,4-dihydroxybenzaldehyde in order to integrate the bio-effectiveness of both azo group and sulfonamide part in the synthesized metal chelates which strongly increase their bio-activities. H_2L and synthesized Cu, Co, Ni, Mn and Zn complexes were characterized applying different analytical and spectral methods. The obtained results revealed that H_2L coordinated with divalent metal ions of copper, cobalt and nickel in a monobasic bidentate mode through the azo group nitrogen, and deprotonated phenolic oxygen whereas H_2L coordinates with Mn(II), and Zn (II) in dibasic tetradentate mode *via* the azo group nitrogen, deprotonated phenolic oxygen, sulfonamide oxygen, and N-atom of thiazole ring. All metal complexes had a tetrahedral geometry around the metal centers. XRD patterns denoted the ligand crystalline and the complexes amorphous natures. TEM images proved the nanosized range of all complex's particles. UV–Vis spectra and viscosity techniques revealed that H_2L and complexes exhibited groove binding mode interactions with DNA. Anticancer efficiency of the ligand and complexes were examined against breast carcinoma cells (MCF-7) and human liver carcinoma cells (HepG-2). Co(II) and Zn(II) complexes displayed the greatest anticancer activity and are very promising candidates for future applications in cancer therapy.

1. Introduction

Bi and multi-nuclear metal chelates have received a great attention due to their unique spectral and magnetic properties as well as their great biological applications [1,2]. Also, the deoxyribonucleic acid (DNA) interaction with these small chelates is an excellent field of interest for chemists and biologists [3,4]. The interactions between transition metal complexes and nucleic acids have received extraordinary attentiveness. This is attributed to their significance in the development of new compounds for medicine and biotechnology [5,6]. Furthermore, many inorganic scientists are interested in designing more efficient, site-precise, less toxic, less expensive, and preferably non-covalently bound anticancer agents [7,8]. In this task, a novel approach is appeared involve designing other metal complexes rather than platinum. For synthesizing inexpensive complexes, metals of the first transition series such as zinc, copper, nickel, cobalt, and manganese, which are widely biologically applicable metals indifferent biomolecules with important physiological activities [9,10], have been reported.

Based on all these facts, the main aims of this work involve the synthesis, structural investigation, anticancer activities, and DNA binding affinity studies of five nanosized mono- and homobi-nuclear complexes of bivalent copper, cobalt, nickel, manganese and zinc ions derived from sulfathiazole azo dye ligand, as a subsequent step for their prospective therapeutic uses as anticancer drugs in the future studies. The active coordination centers in the current azo dye will be investigated and the geometric arrangement around the metal centers will be inspected. The crystalline nature and the size of complexes'

* Corresponding author at: Department of Chemistry, Faculty of Applied Science, Umm Al-Qura University, Makkah, Saudi Arabia.
E-mail address: maa_kassem@hotmail.com (M.A. Kassem).

https://doi.org/10.1016/j.inoche.2019.107496
Received 22 June 2019; Received in revised form 22 July 2019; Accepted 24 July 2019
Available online 04 August 2019
1387-7003/

particles will be studied. As a result of the great importance of examining the entanglement of the chelates with DNA in the evolution of new reagents for medicinal and biotechnological applications, the mode of binding of the characterized compounds with DNA will be investigated.

2. Experimental

2.1. Preparation of sulfathiazolyle azo dye ligand (H_2L)

The H_2L ligand (H_2L = 4-(2,4-dihydroxy-5-formylphen-1-ylazo)-N-thiazol-2-yl-benzenesulfon amide) was prepared applying the following procedures [8]. 4-Amino-N-(1,3-thiazol-2-yl)benzene-sulfonamide (5.10 g, 0.02 mol) suspended in a HCl/H_2O mixture solution (30.0 mL HCl/30.0 mL H_2O) was heated to 75 °C until forming a clear sulfonamide solution. This solution was cooled bellow 5 °C and imperiled to diazotization using a freshly prepared sodium nitrite ($NaNO_2$) solution (3.0 g in 15 mL H_2O) to form solution A. A 2,4-dihydroxybenzaldehyde (2.76 g, 0.02 mol) was dissolved in a strong alkaline NaOH solution (3.2 g in 20 mL H_2O) to form solution B. The formed diazonium salt (solution A) was added drop-wise with contentious stirring to solution B within 30 min. at ~0 °C using an ice bath. The acquired reddish brown H_2L azo dye precipitate was separated by filtration (by the aid of Whatman filter paper No. 40) and washed several times with dist. H_2O then absolute ethanol. Finally, H_2L was recrystallized from absolute ethanol (Fig. 1S).

2.2. Synthesis of nanosized metal complexes

The nanosized transition metal complexes were synthesized applying the well-known reflux-precipitation method. Typically, 2 mM of different metals salts [$CuCl_2{\cdot}2H_2O$ (0.3410 g), $CoCl_2{\cdot}6H_2O$ (0.4759 g), $NiCl_2{\cdot}6H_2O$ (0.4754 g), $MnCl_2{\cdot}4H_2O$ (0.3958 g), and/or $ZnSO_4{\cdot}H_2O$ (0.3589 g), dissolved in 30 mL 50% (V/V) H_2O-C_2H_5OH mixture] were added drop-wise with constant stirring into an ethanolic solution containing 1 mM of the prepared sulfathiazole azo dye, H_2L (0.4044 g). The obtained solutions (from mixing) were refluxed for 10–14 h over water bath after addition of 0.5 mL of triethylamine. Both the presence of triethylamine as a basic medium and contentious stirring enhance the formation of nanosized complexes. The metal chelates formed during the reaction were filtered off and washed by both ethanol and ether. The obtained products were desiccated in a vacuum over $CaCl_2$ (anhydrous). The purity of the formed chelates was tested by the thin layer chromatographic (TLC) technique. The investigation of all synthesized compounds and apparatus applied were the same as given before [8]. Using the well-known recommended techniques [11], the *in-vitro* antitumor activity of all inspected compounds was examined. Binding modes of SS-DNA with the synthesized H_2L besides its prepared complexes (**1–5**) was studied as previously described [10,12].

3. Results and discussion

3.1. Micro-analysis and molar conductivity studies

The results gained for element contents from micro-analysis of sulfathiazole azo dye (H_2L) and all complexes (**1–5**) are in a good agreement with the suggested molecular formulae of the synthesized compounds. The data presented in Table 1 supported the formation of 1:1 (M:L) stoichiometry for Cu(II), Co(II), and Ni(II) complexes and 2:1 (M:L) stoichiometry for Mn(II), and Zn(II) complexes. The molar conductance values achieved for complexes **1–5** were found to be within a 12.8–24.7 $\Omega^{-1}\,cm^2\,mol^{-1}$ range and confirmed the non-electrolytic nature of all complexes under inspection [13].

3.2. Investigation of the ligand to metal binding modes

The FT-IR spectra of the prepared chelates **1–5** are recorded and compared with IR spectra of $H_2L$to find out the coordination sites of H_2L ligand that contribute in bonding with the selected metal ions under consideration (Fig. 2S). The significant bands in ligand spectrum are used to help us in deciding these sites. These peaks frequently exhibited changes either in their shapes and positions or in their intensities while some of them disappear upon complex formation. The important IR bands for the H_2L azo dye ligand and its complexes **1–5** are presented in Table 2. The IR spectrum of the free ligand exhibited a broad band at 3410 cm^{-1} attributed to the stretching mode of intramolecular hydrogen bond of OH [14] and a band at 3145 cm^{-1} assigned to ν_{NH}. The broad bands within 3417–3430 cm^{-1} range appeared in all considered chelates are assigned to the ν_{OH} of solvent molecules combined with the inspected complexes. The stretching vibrational band at 1424 cm^{-1} for free H_2L which referred to $\nu_{N=N}$ was shifted significantly to higher wavenumbers by 16–34 cm^{-1} upon complex formation with the studied metals. These observed shifts give clear evidence of the contribution of nitrogen of azo group in chelation with the metal ions. Another band, found at 1290 cm^{-1} for H_2L, was ascribed to $\nu_{C\text{-}O}$ bond. Upon chelation between H_2L and the metal ions under consideration the position and intensity of this band varied clearly indicating the involvement of the α-OH in chelation through [H^+] dislocation; excluding Zn(II) complex, in which the OH group was coordinated to zinc ion. Also, the band observed at 1527 cm^{-1} for H_2L was assigned to $\nu_{C=N}$ bond of thiazole ring. This band manifested nearly at the same position as the ligand in the spectra of complexes **1**, **2** and **3** indicating that this group is not taking part in complex formation. The shift in this band in the spectra of complexes **4** and **5** is attributed to the participation of $\nu_{C=N}$ in complex formation. The IR spectra of the complexes displayed new non-ligand bands within 575–569 and 459–409 cm^{-1} ranges due to ν(M—O) and ν(M—N), respectively, supporting the coordination of these atoms with the metal ions [15].

3.3. Magnetic moment and electronic spectral studies

For detection of the geometric arrangements of the prepared metal chelates, the electronic absorption (UV–Vis) spectral analysis is considered as one of the most vital tools for this purpose. Also, electronic absorption spectra play a useful role in declaring the coordination between metallic sites and constituent atom of the reacted chelate. The UV/Vis spectra of the H_2L ligand and its chelates **1–5** were measured applying the Nujol mull technique within 200–800 nm range. For the Zn(II) complex, and as predicted, its electronic spectrum did not present any valuable information about its stereochemistry. It was also found to be diamagnetic in nature because d^{10} system of zinc ion which has no unpaired electrons. The obtained spectra of Zn(II) complex showed two spectral peaks at 457 and 546 nm. These two peaks were referred to charge transfer (CT) transitions. Comparing with the obtained complex peaks, the noticeable variations in H_2L peaks are considered a strong evidence for binding between Zn(II) and H_2L ligand. Two peaks in visible region at 444 and 571 nm were observed in case of Mn(II) chelate which attributed to $^6A_1 \rightarrow {}^4T_2$ (G) and $^6A_1 \rightarrow {}^4T_1$(G) transitions, respectively. The magnetic moment of such compound was 5.21 BM which is lower than the magnetic moment value of 5 unpaired referring to metal-metal interactions [16]. For Ni(II) chelate, its electronic spectrum showed three absorption bands at 488, 590 and 732 nm assigned to $^3T_1(F) \rightarrow {}^3T_1(P)$, $^3T_1(F) \rightarrow {}^3A_2(F)$ and $^3T_1(F) \rightarrow {}^3T_2(F)$ transitions. These electronic transitions and a value of 3.44 B.M of magnetic moment are harmonious with a tetrahedral geometry of Ni(II) chelate. For Co(II) chelate, two evident peaks were observed at 547 & 752 nm referring to $^4A_2 \rightarrow {}^4T_1$ (υ_2) &$^4A_2 \rightarrow {}^4T_1$(P) ($\upsilon_3$) transitions, respectively. These transitions support the four coordinate tetrahedral environment around Co(II) ion [17]. Furthermore, the magnetic moment value of 4.27 BM is greater than theoretic spin only value for Co(II) complexes,

Table 1
Physical properties and micro-analytical data of sulfathiazole azo dye, H_2L, and complexes **1–5**.

Comp. no	Molecular formula (Empirical formula)	Color (Mol. wt.)	M. p. (Yield)	Microanalysis, Calc. (found) %		
				C%	H%	N%
H_2L	$C_{16}H_{12}N_4O_5S_2$	Reddish brown	175	47.52	2.99	13.85
		(404.42)	(84)	(47.49)	(3.06)	(13.92)
1	$[LCuCl(H_2O)]0.5MeOH$	Deep red	> 300	36.94	2.82	10.44
	$C_{16.5}H_{15}ClCuN_4O_{6.5}S_2$	(536.45)	(70)	(36.87)	(2.48)	(10.37)
2	$[LCoCl(H_2O)]H_2O$	Reddish brown	> 300	36.00	2.83	10.50
	$C_{16}H_{15}ClCoN_4O_7S_2$	(533.83)	(76)	(36.12)	(2.75)	(10.43)
3	$[LNiCl(H_2O)]2H_2O$	Reddish brown	> 300	34.84	3.11	10.16
	$C_{16}H_{15}ClNiN_4O_7S_2$	(551.6)	(67)	(34.76)	(3.32)	(10.71)
4	$[LMn_2Cl(H_2O)_2]MeOH$	Deep red	> 300	31.35	2.79	8.60
	$C_{17}H_{18}Cl_2Mn_2N_4O_8S_2$	(651.26)	(76)	(31.35)	(2.33)	(9.13)
5	$[LZn_2(SO_4)_2]MeOH$	Dark brown	> 300	26.89	2.12	7.38
	$C_{17}H_{16}N_4O_{14}S_4Zn_2$	(759.35)	(65)	(26.53)	(2.12)	(7.31)

Table 2
Essential IR spectral bands for H_2L and complexes **1–5** with their assignments.

Comp.	ν(OH)	ν(NH)	ν(C=N)	ν(N=N)	ν(C—O)	ν(M—O)	ν(M—N)
H_2L	3410	3145	1527	1424	1290	–	–
1	3430	3237	1529	1458	1281	569	430
2	3417	3221	1528	1449	1265	574	416
3	3417	3229	1529	1449	1270	572	409
4	3418	–	1533	1440	1258	575	459
5	3422	3236	1534	1454	1261	574	457

revealing the orbital participation of Co(II) complexes [18]. Looking to the measured electronic absorption spectrum in case of Cu(II) complex, a broad peak at 757 nm was noticed which ascribed to $^2B_{1g} \rightarrow {}^2A_{1g}$ supporting square-planar geometrical configuration around the Cu(II) ion. The peak existing at 398 nm is imputed to $n \rightarrow \pi^*$ transition within the ligand moiety, whereas the band appeared at 469 nm is corresponding to LMCT. Magnetic moment of Cu(II) complex was determined and found to be 1.77 BM. This value is nigh the range of the spin-allowed values expected for one unpaired electron (1.72 BM), supporting the electronic spectral results [19].

3.4. Thermal gravimetric analysis (TGA)

As it is well known through most scientific literature [20], the thermo-gravimetric analysis (TGA) technique is considered as one of the most important provenances for supporting the molecular structure of most compounds particularly solid metal complexes. TGA provides explicit data about the thermal degradation steps of metal complexes in addition to the final remaining products of their thermal decompositions [21]. It has a high significant in identifying the sorts and percentages of water and/or solvent molecules besides the anionic groups attached to the outer-sphere metal complexes. So, the thermal gravimetric analysis of the solid complexes under interest (**1–5**) were performed and studied. The decomposition stages, temperature ranges, and computed and experimental weight losses of complexes **1–5** are presented in Table 1S and the TG curves are showed in Fig. 3S. Analysis of the TG thermograms of the five complexes proved that the decomposition of these complexes occurred in three (complex **5**) or four (complexes **1**, **2**, **3** and **4**) successive thermal decomposition steps. In the first step of decomposition, the lattice solvent (water or methanol) was evaporated. The second step of thermal degradation is imputed to the forfeiture of coordinated water molecules and OH^- ion; except for complex **5** while this step involved the loss of SO_2 moiety of connected sulfate group. The third step of decomposition was assigned to the loss of coordinated anion (Cl^- or SO_4^{2-}) along with partial or complete degradation of the organic ligand. For complexes **1–4**, the fourth and the last step of decomposition included the forfeiture of the remnant fraction of the organic ligand resulting in forming the metal oxide or just the metal as a residue. The thermal decomposition of compound **4**, as illustrative example, can be illustrated by the following schemes:

$$[LMn_2Cl(H_2O)_2]MeOH \xrightarrow[-4.5\ (calcd.\ 4.91\%)]{23-73^\circ C} [LMn_2Cl(H_2O)_2]$$

$$[LMn_2Cl(H_2O)_2] \xrightarrow[-8.42\ (calcd.\ 8.13\%)]{73-235^\circ C} [LMn_2Cl]$$

$$[LMn_2Cl] \xrightarrow[-23.57\ (calcd.\ 23.66\%)]{235-428^\circ C} \text{Intermediate 1}$$

$$\text{Intermediate 1} \xrightarrow[-47.04\ (calcd.\ 46.26\%)]{428-784^\circ C} 2Mn$$

As showed previously and as showed in Table 1S, the gained data from the thermal gravimetric analysis for all complexes (**1–5**) undoubtedly confirmed their investigated molecular formulae. Based on data achieved from microanalysis, TGA, electronic and IR spectra, in addition to molar conductance and magnetic moment studies, the models of H_2L ligand and its complexes in different stoichiometry are shown in Fig. 1 & 1S.

3.5. TEM and XRD investigation

Transmittance electron microscopy (TEM) is one of the inherent tools that normally used to analyze enhanced intriguing nanosized metal chelates [22]. It is also, to a great extent, a valuable method for examination of size and shape of solid chelates molecules. Indeed, Fig. 2 represents the high-resolution TEM pictures for all considered chelates. TEM images allowed us to provide a set of data corresponding to the molecule size, homogeneity, surface morphology, and microstructure for the prepared compounds (**1–5**). The obtained images showed particular shapes of molecules. A uniform and homogeneity of surface morphology was observed for the inspected complexes. As also can be seen, the spherical features appearing in images (Fig. 2) can be assigned to the presence of symmetrical circular anions into the coordination sphere. Interestingly, this can be analyzed by the various piling up of diverse units presenting a poly crystalline character. On the other hand, the blackish zones showed up in the acquired pictures might be ascribed to the grouping of extremely small size complex particles. Compared to the inset scale bar, it should be noted that the observed complex diameters for all prepared chelates (**1–5**) were found to be in the range of nano-meter scale. A particle size values of 43.58, 52.41, 52.27, 24.46 and 34.61 nm for Cu(II), Co(II), Ni(II), Mn(II) and Zn complexes **1–5**, respectively, were found. Such nano-metric scale values of the current complexes generally improve the biological efficacy when compared with the bulk analogue. This interesting character rationalizes the porousness natural cells *via* cell films. Great attention toward the novel

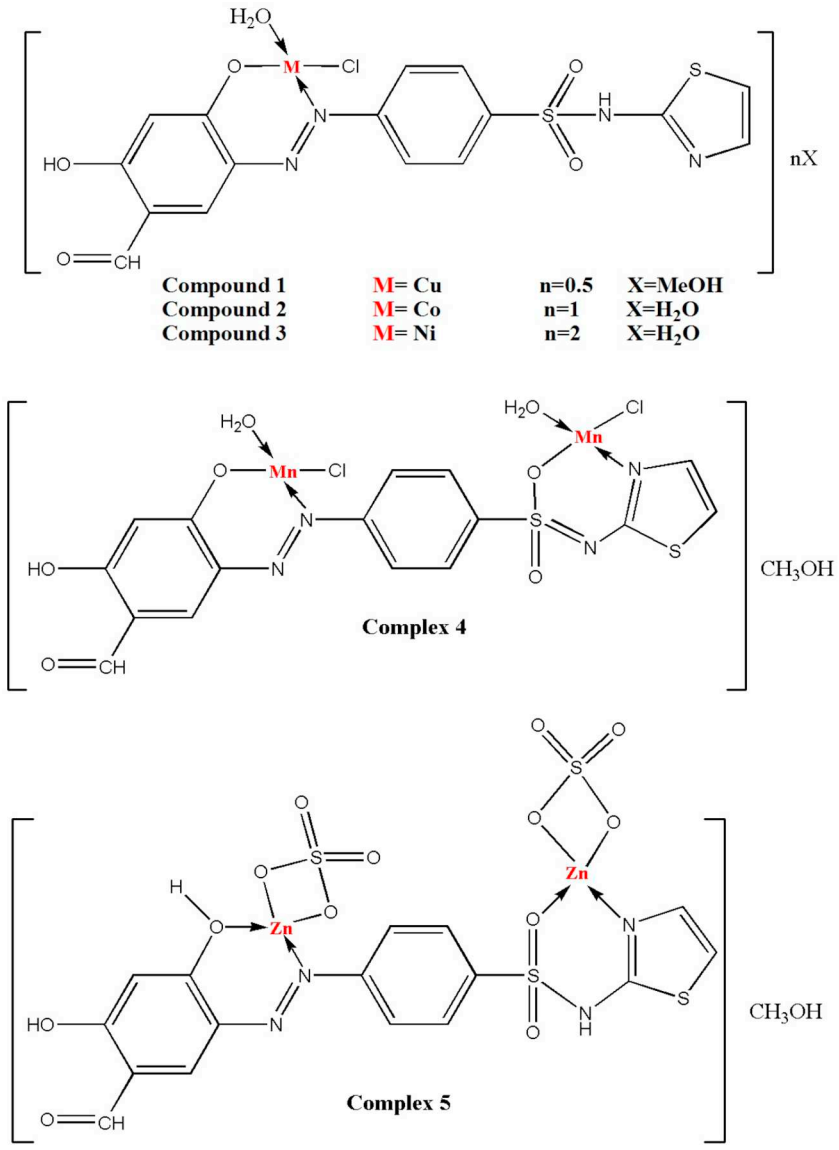

Fig. 1. Molecular structures of the investigated complexes **1**–**5**.

nanosized metal complexes can lead to enormous progress and a wonderful scale of possible technological development due to their recognized useful properties [23].

XRD (X-ray powder diffraction) is considered indisputably as one of the most significant techniques which can display beneficial information regarding microcrystalline nature of the inspected compounds

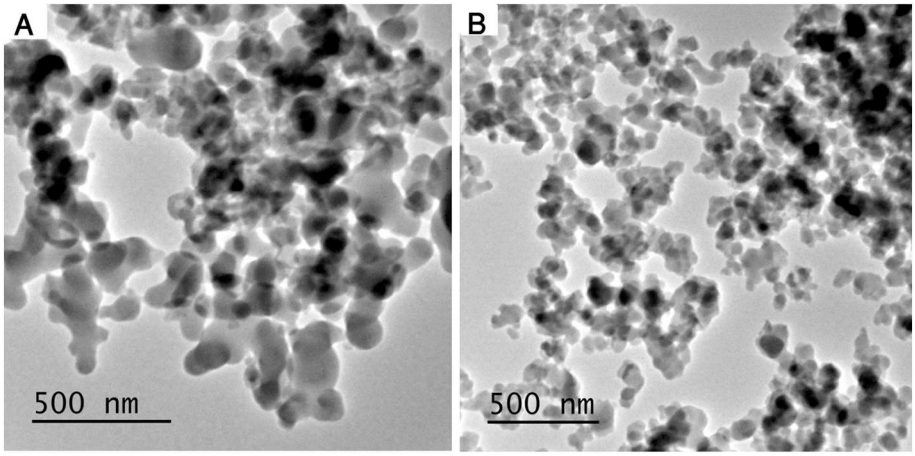

Fig. 2. TEM images of Co(II) complex **2** (**A**) and Ni(II) complex **3** (B).

[24]. Also, it is usually applied to better visualize the lattice dynamics of the solid materials. The x-ray diffraction patterns corresponding to the H_2L ligand and related complexes **1–5** were performed within a wide range of scattering angles ($0° < 2\theta < 90°$). Furthermore, the diffraction patterns of H_2L ligand are completely different in comparison with the corresponding metal complexes (Fig. 4S), as an extra supporting evidence for the formation of complexes [25]. The H_2L ligand patterns showed high crystallinity whereas the inspected complexes **1–5** displayed amorphous nature. This can be assigned to infrequent configuration for rapid precipitation process of the solid frameworks. Such state, amorphous, is the predominating one if the complexation process is prompt and/or the produced compound is cooled speedily. Moreover, many constituents in the complex's structures do not have capability to be displayed within a crystal lattice. So, they are precipitated in intrinsically amorphous state. The amorphous nature of the investigated complexes may also reflect the immeasurably small sizes for the aggregates which are in the nano-metric range as verified through TEM analysis [26].

3.6. Investigation of DNA binding modes

3.6.1. Electronic absorption (UV–Vis) spectral studies

Ultraviolet and visible (UV–Vis) absorption spectroscopy is a basic technique which is exercised for evaluating the coupling method of the test reagents with DNA [12,27]. The spectral studies were managed through mixing fixed concentrations (*i.e.* 50 μM) of both prepared complexes (**1–5**) and ligand H_2L with varied concentrations of DNA (from 5.0×10^{-6} to 45.0×10^{-6} M). The Electronic absorption spectra were measured against a blank containing the same amount of DNA. The measured spectra for the binding ability of each of H_2L & Zn(II) complex **5** with SS-DNA are showed in Figs. 3 & 5S. The actual binding constants (K_b) corresponding to the association between the studied ligand alongside its chelates and DNA are exactly calculated utilizing the CT absorbance peaks. As shown in Figs. 3 & 5S, due to the combination between H_2L and DNA, a clear hypochromism was occurred for the charge transfer peak which, as observed, has a slight shift in λ_{max}; sometimes no shift is noticed. This observation can be attributed to the intercalative type of interaction among the considered chelates and nucleotide pairing [28]. The extent of hypochromism is ordinarily matching with the extent of intercalation. It is important to note that the hyperchromism presents another obvious spectral feature. It indeed informs us about the fracturing of the secondary DNA structure [29]. The observed spectral feature for the CT band appearing at 433, 429, 360, 438, 450 and 447 nm, respectively, for H_2L and complexes **1–5** with DNA, showed hyperchromism of 25.1, 12.33, 40.5, 19.68, 27.4 and 52.5%, respectively, indicating a groove binding mode [12]. The values of binding constant of compounds with DNA, K_b were determined using the following equation:

$$\frac{[DNA]}{(\varepsilon_a - \varepsilon_f)} = \frac{[DNA]}{(\varepsilon_b - \varepsilon_f)} + \frac{1}{[K_b(\varepsilon_b - \varepsilon_f)]}$$

where [DNA] represent the concentration of DNA solution in the base pairs, while ε_a, ε_f and ε_b corresponds respectively to, the absorption coefficient which equal to A_{obs}/[compound], the extinction coefficient of the unbounded and the compound in a fully bound state to DNA. K_b is determined when plotting [DNA]/(ε_a–ε_f) *versus* [DNA] from the ratio of slope to intercept, knowing that the plots are linear with slope = 1/(ε_b–ε_f) and intercept = 1/K_b (ε_b–ε_f). The obtained values of the binding constant (K_b) were found to be 9.4×10^3, 8.8×10^3, 1.9×10^4, 1.7×10^4, 1.3×10^4, and 1.7×10^4 corresponding to the association of DNA with H_2L, **1**, **2**, **3**, **4**, and **5**, respectively. Interestingly, the determined K_b values of the studied compounds indicate that these compounds show a reasonable binding ability compared to the commonly reported ethidium bromide intercalating agent [12].

3.6.2. Viscosity studies

The optical tools, such as UV–Vis spectra seem to be not sufficient to evaluate the type of interaction between compounds and DNA. Among the proposed tools to better describe this interaction, hydrodynamic tools such as viscosity have shown to provide a great sensitivity toward DNA length and therefore introduces large accuracy to any change in DNA length. Thus, viscosity is probably an influential tool to estimate the coupling mode between DNA and the examined compounds. Herein, the viscosity of a fixed DNA concentration was determined using different concentrations of the tested compounds (ligand H_2L, and complexes **1–5**). In literature, ethidium bromide [EB], as a reference example of intercalators usually results in a significant augmentation in DNA viscosity due to the increase in the distance separating the intercalation sites base pairs that result in a final increase in the DNA length [30]. The increasing effect of concentrations of ligand H_2L and complexes **1–5** on the viscosity of SS-DNA was presented in Fig. 4. In addition, the relative viscosity of solution of DNA underwent a slight increase overall the entire range upon increasing the ligand H_2L and compounds **1–5** concentrations suggesting groove binding mode interaction.

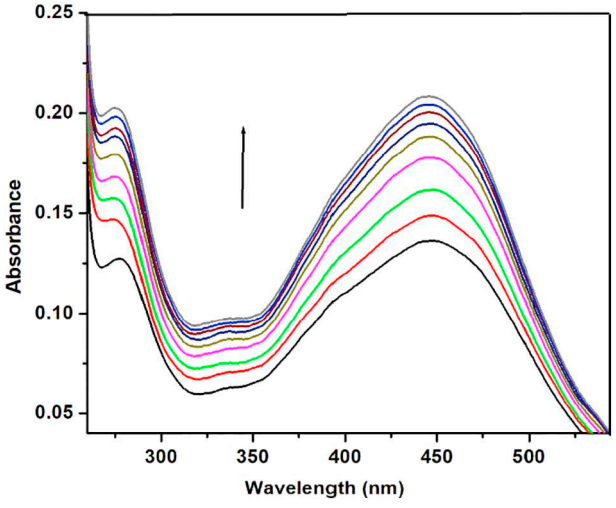

Fig. 3. Electronic absorption spectra of Zn(II) complex (**5**) in the absence and existence of rising quantities of SS-DNA.

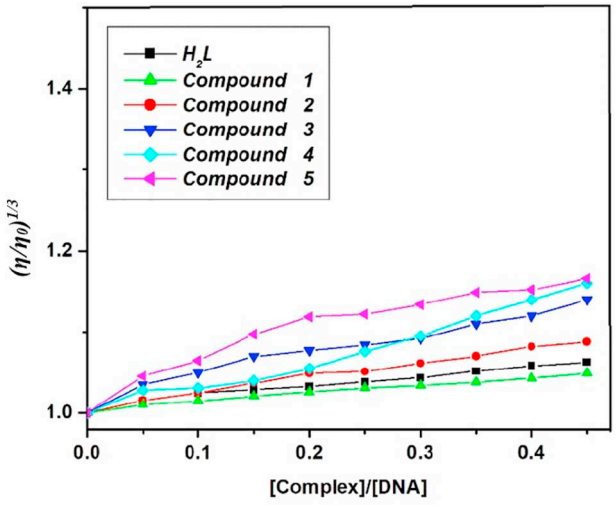

Fig. 4. Effect of increasing concentrations of H_2L and complexes **1–5** on the viscosity of SS-DNA.

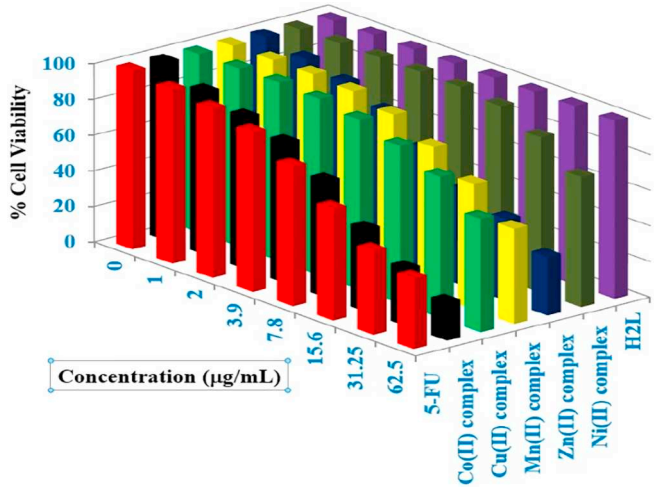

Fig. 5. The *in-vitro* antitumor activity of H_2L, and its complexes **1–5** toward MCF-7 cell lines, in comparison with the applied standard 5-flurouracil.

3.7. Anticancer efficiency assays

Chemotherapy is noticed as a primary methodology for limited and metastasized cancer treating. However, the discovery of novel and efficient anticancer compounds seems to be necessary to progress the results that represents a hope for enormous number of patients that relapse when treated with current and known cancer therapeutic agents [30–33]. One important objective of the current study is assessing the anticancer activities of ligand H_2L and complexes **1–5** against human *Hepatocellular* carcinoma cell lines (HepG-2 cells) and human *breast* cancer cell lines (MCF-7 cells). The choice of cells here is not arbitrary since selected HepG-2 and MCF-7 represent the most common cells among other several types of carcinomas. On the other hand, it is well known that the growth inhibitory activities and antitumor activity were both specified by IC_{50} parameter [31]. Indeed, IC_{50} refers to the concentration of scanned component that, at the same applied conditions, decreases the cell growth by a percentage of 50%. Every result obtained was obtained from the mean of triple measurements and subsequently identified as M ± SD. The IC_{50} values obtained in this work for all investigated compounds are assembled in Table 2S. The *in-vitro* antitumor activity is afforded in Fig. 6S in which we present the activity of H_2L and its chelates **1–5** against HepG-2 cell lines, compared with the applied standard drug cisplatin (cis-DDP). It is clear from the displayed figures that our compounds have an inhabitation behavior against HepG-2 in the order; H_2L ≈ manganese complex **4** ≈ zinc complex **5** < nickel complex **3** < copper complex **1** < cobalt complex **2**. Interestingly, it is obvious that Co(II) complex **2** showed the highest activity with a value of 179.45 µM (95.80 µg/ml) of IC_{50} compared with the applied standard drug cis-DDP which has a value of 40.76 µM (12.23 µg/ml). Furthermore, the complex **2** exhibited relatively low activity when compared with the previous findings for azo pyrazolone complexes which has IC_{50} = 24.43 µM (10.73 µg/ml) [32], and complexes of aryl hydrazonos with IC_{50} reached 32.25 µM (11.80 µg/ml) [33], contra HepG-2 cell lines. Fig. 5 shows the *in-vitro* antitumor efficiency of sulfathiazole azo dye ligand, H_2L, and related complexes (**1–5**) against MCF-7 cells comparable with 5-flurouracil, the applied standard drug. As we can see, nearly most investigated compounds exhibited an inhibition of cell viability and increased the anticancer activity against MCF-7 according to following the order; H_2L < nickel complex **3** < copper complex **1** < manganese complex **4** < cobalt complex **2**. The given results clarify the predominant role of both nature and properties of metal in limiting the anticancer activity of the metallic compounds [34,35]. The very promising data is obtained for Co (II) and Zn(II) complexes which displayed IC_{50} equal 26.41 µM (14.10 µg/ml) and 30.28 µM (23.00 µg/ml), respectively. These values are greater than the IC_{50} of 5-flurouracil, the applied standard drug which has IC_{50} = 215.26 µM (28 µg/ml). This means that these compounds are much more efficient than the applied standard 5-flurouracil against MCF-7 cells. Comparing the obtained results with the literature values confirmed that IC_{50} of Co(II) complex **2** is much greater than the previous findings obtained for azo pyridine complexes, IC_{50} reached 31.66 µM (19.40 µg/ml) [36], toward the same type cancer cells. Hence, Co(II) and Zn(II) complexes inspected in this study are considered quite promising anticancer agents which might be applied as new curing agents from cancer after further medicinal studies.

4. Conclusion

This work described the synthesis of five new nanosized mono- and homobi-nuclear complexes based on 4-(2,4-dihydroxy-5-formylphen-1-ylazo)-N-thiazol-2-yl-benzenesulfonamide (H_2L) ligand aiming to develop new promising anticancer agents. In order to integrate the bio-effectiveness of both sulfonamide part and azo group in the synthesized metal complexes which strongly enhance their bio-activities, H_2L was prepared by coupling 2,4-dihydroxybenzaldehyde with the diazonium salt of sulfathiazole. The ligand and its Cu(II), Co(II), Ni(II), Mn(II), and Zn(II) complexes were inspected using different analytical and spectral techniques. The results demonstrated that H_2L coordinates with Mn(II), and Zn(II)in a dibasic tetradentate mode through one azo group nitrogen, deprotonated phenolic oxygen, sulfonamide oxygen, and N-atom of thiazole ring, whereas H_2L coordinates with Cu(II), Co(II), and Ni(II)in a monobasic bidentate mode through one azo group nitrogen, and deprotonated phenolic oxygen. All complexes exhibited tetrahedral arrangement surrounding the metal ions. TEM images asserted the nanometric size of the studied complex's particles. XRD patterns confirmed crystalline nature of ligand and the amorphous nature of the studied complexes. Electronic absorption and viscosity measurements denoted that H_2L and complexes exhibited groove binding mode interactions with DNA. Anticancer activity screening proved that Co(II) and Zn(II) complexes, with IC_{50} values 26.42 µM (14.10 µg/ml) and 30.28 µM (23.00 µg/ml), are quite hopeful anticancer agents which can be applied as a novel drugs after deep medicinal studies in the future.

Acknowledgement

This paper contains the results and findings of a research project that is funded by King Abdulaziz City for Science and Technology (KACST) Grant No. 37-175.

Appendix A. Supplementary material

Supplementary data to this article can be found online at https://doi.org/10.1016/j.inoche.2019.107496.

References

[1] P.A. Kobielska, R. Telford, J. Rowlandson, M. Tian, Z. Shahin, A. Demessence, V.P. Ting, S. Nayak, Polynuclear complexes as precursor templates for hierarchical microporous graphitic carbon: an unusual approach, ACS Appl. Mater. Interfaces 10 (2018) 25967–25971, https://doi.org/10.1021/acsami.8b10149.
[2] F.A. Saad, A.M. Khedr, Greener solid state synthesis of nano-sized mono and homo bi-nuclear Ni(II), Co(II), Mn(II), Hg(II), Cd(II) and Zn(II) complexes with new sulfa ligand as a potential antitumour and antimicrobial agents, J. Mol. Liq. 231 (2017) 572–579, https://doi.org/10.1016/j.molliq.2017.02.046.
[3] A.A. Almaqwashi, T. Paramanathan, I. Rouzina, M.C. Williams, Mechanisms of small molecule-DNA interactions probed by single-molecule force spectroscopy, Nucleic Acids Res. 44 (2016) 3971–3988, https://doi.org/10.1093/nar/gkw237.
[4] C.Y. Lee, H.Y. Kim, S. Kim, K.S. Park, H.G. Park, A simple and sensitive detection of small molecule–protein interactions based on terminal protection-mediated exponential strand displacement amplification, Analyst 143 (2018) 2023–2028, https://doi.org/10.1039/C8AN00099A.
[5] P. Zhao, S. Zhai, J. Dong, L. Gao, X. Liu, L. Wang, J. Kong, L. Li, Synthesis, structure, DNA interaction, and sod activity of three nickel(II) complexes containing L-phenylalanine Schiff base and 1,10-phenanthroline, Bioinorg. Chem. Appl. 2018 (2018)

8478152, https://doi.org/10.1155/2018/8478152.
[6] A. Erxleben, Interactions of copper complexes with nucleic acids, Coord. Chem. Rev. 360 (2018) 92–121, https://doi.org/10.1016/j.ccr.2018.01.008.
[7] A. Hussain, M.F. AlAjmi, M. Rehman, A.A. Khan, P.A. Shaikh, R.A. Khan, Evaluation of transition metal complexes of benzimidazole-derived scaffold as promising anticancer chemotherapeutics, Molecules 23 (2018) 1232–1249, https://doi.org/10.3390/molecules23051232.
[8] F.A. Saad, H. El-Ghamry, M.A. Kassem, A.M. Khedr, Nano-synthesis, biological efficiency and DNA binding affinity of new homo-binuclear metal complexes with sulfa azo dye-based ligand for further pharmaceutical applications, J. Inorg. Organomet. Polym. Mater. 29 (2019) 1337–1348, https://doi.org/10.1007/s10904-019-01098-z.
[9] M.A. Malik, O.A. Dar, P. Gull, M.Y. Wani, A.A. Hashmi, Heterocyclic Schiff base transition metal complexes in antimicrobial and anticancer chemotherapy, Med. Chem. Commun. 9 (2018) 409–436, https://doi.org/10.1039/C7MD00526A.
[10] F.A. Saad, H.A. El-Ghamry, M.A. Kassem, Synthesis, structural characterization and DNA binding affinity of new bioactive nano-sized transition metal complexes with sulfathiazole azo dye for therapeutic applications, Appl. Organometal. Chem. 33 (2019) e4965, , https://doi.org/10.1002/aoc.4965.
[11] S.M. Gomha, S.M. Riyadh, E.A. Mahmmoud, M.M. Elaasser, Synthesis and anticancer activity of arylazothiazoles and 1,3,4-thiadiazoles using chitosan-grafted-poly (4-vinylpyridine) as a novel copolymer basic catalyst, Chem. Heterocycl. Compd. 51 (2015) 1030–1038, https://doi.org/10.1007/s10593-016-1815-9.
[12] M. Gaber, N.A. El-Wakiel, H. El-Ghamry, S.K. Fathalla, Synthesis, spectroscopic characterization, DNA interaction and biological activities of Mn(II), Co(II), Ni(II) and Cu(II) complexes with [(1H- 1,2,4-triazole-3-ylimino)methyl]naphthalene-2-ol, J. Mol. Struct. 1076 (2014) 251–261, https://doi.org/10.1016/j.molstruc.2014.06.071.
[13] W.J. Geary, The use of conductivity measurements in organic solvents for the characterisation of coordination compounds, Coord. Chem. Rev. 7 (1971) 81–122, https://doi.org/10.1016/S0010- 8545(00)80009-0.
[14] K. Nakamoto, Infrared Spectra of Inorganic and Coordination Compounds, Wiley, New York, 1986.
[15] K. El-Baradie, R. El-Sharkawy, H. El-Ghamry, K. Sakai, Synthesis and characterization of Cu(II), Co(II) and Ni(II) complexes of a number of sulfa drug azo dyes and their application for wastewater treatment, Spectrochim. Acta A 121 (2014) 180–187, https://doi.org/10.1016/j.saa.2013.09.070.
[16] W. Al Zoubi, A.A.S. Al-Hamdani, S.D. Ahmed, Y.G. Ko, Synthesis, characterization, and biological activity of Schiff bases metal complexes, J. Phys. Org. Chem. 31 (2017) e3752, , https://doi.org/10.1002/poc.3752.
[17] A.A. Osowole, E.J. Akpan, Synthesis, spectroscopic characterisation, in-vitro anticancer and antimicrobial activities of some metal(II) complexes of 3-(4,6-dimethoxy pyrimidinyl) iminomethyl naphthalen-2-ol, Eur. J. Appl. Sci. 4 (2012) 14–20 https://pdfs.semanticscholar.org/53fb/ff7a0fd3e5e34de1767c8b81171723d47375.pdf.
[18] M.M. Al-Ne'aimi, M.M. Al-Khuder, Synthesis, characterization and extraction studies of some metal (II) complexes containing (hydrazoneoxime and bis-acylhydrazone) moieties, Spectrochim. Acta A 105 (2013) 365–373, https://doi.org/10.1016/j.saa.2012.10.046.
[19] P.N. Patel, D.J. Patel, H.S. Patel, Synthesis, spectroscopic, thermal and biological aspects of drug-based copper(II) complexes, Appl. Organomet. Chem. 25 (2011) 454–463, https://doi.org/10.1002/aoc.1786.
[20] G.Q. Zhong, J. Shen, Q.Y. Jiang, Y.Q. Jia, M.J. Chen, Z.P. Zhang, Synthesis, characterization and thermal decomposition of SbIII-M-SbIII type trinuclear complexes of ethylenediamine-N,N,N′,N′-tetraacetate (M:Co(II), La(III), Nd(III), Dy(III)), J. Therm. Anal. Calorim. 92 (2008) 607–616, https://doi.org/10.1007/s10973-007-8579-5.
[21] M. Badea, A. Emandi, D. Marinescu, E. Cristurean, R. Olar, A. Braileanu, P. Budrugeac, E. Segal, Thermal stability of some azo-derivatives and their complexes, J. Therm. Anal. Calorim. 72 (2003) 525–531, https://doi.org/10.1023/A:1024517430630.
[22] J.K. Hui, M.J. MacLachlan, Metal-containing nanofibers via coordination chemistry, Coord. Chem. Rev. 254 (2010) 2363–2390, https://doi.org/10.1016/j.ccr.2010.02.011.
[23] A. Salimi, J.R. Halla, S. Soltanian, Immobilization of hemoglobin on electrodeposited cobalt-oxide nanoparticles: direct voltammetry and electrocatalytic activity, Biophys. Chem. 130 (2007) 122–131, https://doi.org/10.1016/j.bpc.2007.08.004.
[24] A.A. Fahem, Comparative studies of mononuclear Ni(II) and UO2(II) complexes having bifunctional coordinated groups: synthesis, thermal analysis, X-ray diffraction, surface morphology studies and biological evaluation, Spectrochim. Acta A 88 (2012) 10–22, https://doi.org/10.1016/j.saa.2011.11.037.
[25] F.A. Saad, J.H. Al-Fahemi, H. El-Ghamry, A.M. Khedr, M.G. Elghalban, N.M. El-Metwaly, Elaborated spectral, modeling, QSAR, docking, thermal, antimicrobial and anticancer activity studies for new nanosized metal ion complexes derived from sulfamerazine azodye, J. Therm. Anal. Calorim. 131 (2018) 1249–1267, https://doi.org/10.1007/s10973-017-6598-4.
[26] F.A. Saad, M.G. Elghalban, N. El-Metwaly, H. El-Ghamry, A.M. Khedr, Density functional theory/B3LYP study of nanometric 4(2,4dihydroxy-5-formylphen-1-ylazo)-N-(4-methylpyrimidin-2-yl)benzenesulfonamide complexes: quantitative structure–activity relationship, docking, spectral and biological investigations, Appl. Organomet. Chem. 11 (2017) e3721, https://doi.org/10.1002/aoc.3721.
[27] T. Hirohama, Y. Kuranuki, E. Ebina, T. Sugizaki, H. Arii, M. Chikira, P.T. Selvi, M. Palaniandavar, Copper(II) complexes of 1,10-phenanthroline-derived ligands: studies on DNA binding properties and nuclease activity, J. Inorg. Biochem. 99 (2005) 1205–1219, https://doi.org/10.1016/j.jinorgbio.2005.02.020.
[28] T.R. Li, Z.Y. Yang, B.D. Wang, D.D. Qin, Synthesis, characterization, antioxidant activity and DNA-binding studies of two rare earth(III) complexes with naringenin-2-hydroxy benzoyl hydrazone ligand, Eur. J. Med. Chem. 43 (2008) 1688–1895, https://doi.org/10.1016/j.ejmech.2007.10.006.
[29] N. Chitrapriya, V. Mahalingam, M. Zeller, K. Natarajan, Synthesis, characterization, crystal structures and DNA binding studies of nickel(II) hydrazone complexes, Inorg. Chim. Acta 363 (2010) 3685–3695, https://doi.org/10.1016/j.ica.2010.05.017.
[30] F.H. Li, G.H. Zhao, H.X. Wu, H. Lin, X.X. Wu, S.R. Zhu, H.K. Lin, Synthesis, characterization and biological activity of lanthanum(III) complexes containing 2-methylene–1,10-phenanthroline units bridged by aliphatic diamines, J. Inorg. Biochem. 100 (2006) 36–43, https://doi.org/10.1016/j.jinorgbio.2005.09.012.
[31] S.H. Etaiw, S.A. Amer, M.M. El-Bendary, A mixed valence copper cyanide 3D-supramolecular coordination polymer containing 1,10-phenathorline ligand as a potential antitumor agent, effective catalyst and luminescent material, J. Inorg. Organomet. Polym. Mater. 21 (2011) 662–669, https://doi.org/10.1007/s10904-011-9532-4.
[32] E.A. Bakr, G.B. Al-Hefnawy, M.K. Awad, H.H. Abd-Elatty, M.S. Youssef, New Ni (II), Pd (II) and Pt (II) complexes coordinated to azo pyrazolone ligand with a potent anti-tumor activity: synthesis, characterization, DFT and DNA cleavage studies, Appl. Organomet. Chem. 32 (2018) e4104, , https://doi.org/10.1002/aoc.4104.
[33] A.F. Shoair, A.A. El-Bindary, N.A. El-Ghamaz, G.N. Rezk, Synthesis, characterization, DNA binding and antitumor activities of Cu(II) complexes, J. Mol. Liq. 269 (2018) 619–638, https://doi.org/10.1016/j.molliq.2018.08.075.
[34] M. Gaber, A.M. Khedr, M. Elsharkawy, Characterization and thermal studies of nano-synthesized Mn(II), Co(II), Ni(II) and Cu(II) complexes with adipohydrazone ligand as new promising antimicrobial and antitumor agents, Appl. Organomet. Chem. 31 (2017) 3885–3898, https://doi.org/10.1002/aoc.3885.
[35] X. Riera, V. Moreno, C.J. Ciudad, V. Noe, M. Font-Bardía, X. Solans, Complexes of Pd(II) and Pt(II) with 9-aminoacridine: reactions with DNA and study of their antiproliferative activity, Bioinorg. Chem. Appl. 2007 (2007) 1, https://doi.org/10.1155/2007/98732.
[36] W.H. Mahmoud, F.N. Sayed, G.G. Mohamed, Azo dye with nitrogen donor sets of atoms and its metal complexes: synthesis, characterization, DFT, biological, anticancer and molecular docking studies, Appl. Organomet. Chem. 32 (2018) e4347, , https://doi.org/10.1002/aoc.4347.